Bioorganic & Medicinal Chemistry 22 (2014) 865–873

Contents lists available at ScienceDirect

Bioorganic & Medicinal Chemistry

journal homepage: www.elsevier.com/locate/bmc

Synthesis, docking simulation, biological evaluations and 3D-QSAR study of 5-Aryl-6-(4-methylsulfonyl)-3-(metylthio)-1,2,4-triazine as selective cyclooxygenase-2 inhibitors

Hamid Irannejad [a], Abbas Kebriaieezadeh [b], Afshin Zarghi [c], Farhad Montazer-Sadegh [b], Abbas Shafiee [d], Amir Assadieskandar [e], Mohsen Amini [e,*]

[a] Department of Medicinal Chemistry and Pharmaceutical Sciences Research Center, Faculty of Pharmacy, Mazandaran University of Medical Sciences, Sari, Iran
[b] Department of Pharmacology Toxicology, Faculty of Pharmacy, Tehran University of Medical Sciences, Tehran, Iran
[c] Department of Medicinal Chemistry, Faculty of Pharmacy, Shahid Beheshti University of Medical Sciences, Tehran, Iran
[d] Department of Medicinal Chemistry, Faculty of Pharmacy and Pharmaceutical Sciences Research Center, Tehran University of Medical Sciences, Tehran 14176, Iran
[e] Department of Medicinal Chemistry, Faculty of Pharmacy and Drug Design Development Research Center, Tehran University of Medical Sciences, Tehran 14176, Iran

ARTICLE INFO

Article history:
Received 18 September 2013
Revised 1 December 2013
Accepted 2 December 2013
Available online 11 December 2013

Keywords:
Cyclooxygenase
Inflammatory and analgesic properties
Docking
3D-QSAR
1,2,4-Triazine

ABSTRACT

A series of 5-Aryl-6-(4-methylsulfonyl)-3-(metylthio)-1,2,4-triazine derivatives were synthesized and their COX-1/COX-2 inhibitory activity as well as in vivo anti-inflammatory and analgesic effects were evaluated. All of compounds showed strong inhibition of COX-2 with IC_{50} values in the range of 0.1–0.2 μM and in most cases had stronger anti-inflammatory and analgesic effects than indomethacin at doses 3 and 6 mg/kg. Among them, 5-(4-chlorophenyl)-6-(4-(methylsulfonyl) phenyl)-3-(methylthio)-1,2,4-triazine (**9c**) was the most potent and selective COX-2 compound; its selectivity index of 395 was comparable to celecoxib (SI = 405). Evaluation of anti-inflammatory and analgesic effects of **9c** showed its higher potency than indomethacin and hence could be considered as a promising lead candidate for further drug development. Furthermore, the affinity data of these compounds were rationalized through enzyme docking simulation and 3D-QSAR study by k-Nearest Neighbour Molecular Field Analysis.

1. Introduction

Cyclooxygenase (COX) is an endogenous enzyme that catalyzes the first step in the conversion of arachidonic acid into prostaglandins and thromboxanes. COX is competitively inhibited by a group of drugs known as nonsteroidal anti-inflammatory drugs (NSAIDs) that are used for therapy and management of inflammation and pain. In spite of their beneficial action, their activity is associated with deleterious side effects such as nephrotoxicity and gastric ulcers.[1] Consequently, new NSAIDs with fewer side effects are necessary for safer treatment. A key step in the discovery of novel NSAIDs lacking the deleterious side effects came from the characterization and isolation of two different COX isoforms. Constitutive COX-1, which is responsible for cytoprotective effects involved in maintenance of gastric and renal functions as well as vascular homeostasis, and inducible COX-2, which is expressed only in inflammatory situations.[2,3] So it was understood that the therapeutic anti-inflammatory action of NSAIDs is produced by inhibition of COX-2 while the unwanted side effects arise from inhibition of COX-1 activity. Accordingly, in recent years a great deal of interest has been devoted to the discovery of selective COX-2 inhibitors. Several selective COX-2 inhibitors have been developed and marketed up to now. Among them, celecoxib, valdecoxib and etoricoxib have been clinically validated as anti-inflammatory therapeutics for indications such as acute pain, rheumatoid arthritis and osteoarthritis,[4,5] as well as in treatment of cancer cell lines[6] and neurodegenerative disorders like Alzheimer's and Parkinson's diseases.[7]

Most of the COX-2 inhibitors are characterized by a 1,2-diaryl substituted on a central heterocyclic ring system. Extensive structure–activity studies demonstrated that a SO_2CH_3 or SO_2NH_2 group at the *para* position of one of the aryl rings provides optimum COX-2 selectivity and inhibitory potency. Unfortunately, these compounds are associated with adverse cardiovascular effects such as myocardial infarction, thrombosis and cardiac dysfunction.[8] The most plausible reason for this effect is the suppression of COX-2 dependent prostacyclin which mediate platelet activation and atherogenesis.[9] Therefore, the search for a novel, structurally different and better pharmacodynamic profile of selective COX-2 inhibitors devoid of the noted side effects is still an ongoing need for anti-inflammatory therapy.

* Corresponding author. Tel.: +98 21 66959090; fax: +98 21 66461178.
E-mail address: moamini@sina.tums.ac.ir (M. Amini).

0968-0896/$ - see front matter © 2013 Elsevier Ltd. All rights reserved.
http://dx.doi.org/10.1016/j.bmc.2013.12.002

We have previously reported the design and synthesis of 2-alkylthio-1,5-diarylimidazoles (**1**),[10a] 4-aryl-5-(4-(methylsulfonyl)phenyl)-2-alkylthio-1*H*-imidazole (**2**),[10b] and 3-alkylthio-4,5-diaryl-4*H*-1,2,4-triazoles (**3**)[11] as selective COX-2 inhibitors in which the central ring was imidazole and triazole substituted with alkylthio groups. Herein, as part of our ongoing program, we describe synthesis, docking simulation and 3D-QSAR study of some 3-alkylthio-4,5-diaryl-1,2,4-triazine derivatives (**9**) as selective COX-2 inhibitors (Fig. 1). Furthermore, the biological activity (anti-inflammatory (AI) and analgesic activities) of the synthesized compounds were evaluated in both in vitro and in vivo studies.

2. Results and discussion

2.1. Chemistry

Phenylacetic acid derivatives were converted to the corresponding compounds (**5**) in the presence of trifluoroacetic acid anhydride, phosphoric acid and thioanisole.[12] Then sulfur atom was oxidized to the sulfonyl by oxone in THF/MeOH and the resulting material (**6**) was reacted with sodium methoxide and then butyl nitrite to produce compound (**7**). Triazine ring closure (**8**) was performed with thiosemicarbazide in acidic water[13] and the final compound (**9**) was obtained through the reaction of compound (**8**) in the presence of methyl iodide and triethylamine in methanol[14] (Scheme 1).

2.2. Inhibition of cyclooxygenase

The synthesized compounds (**9a**–**e**) were all evaluated for their inhibitory activity against COX-1 and COX-2 enzymes. Analysis of biological data showed that all compounds are strong inhibitors of COX-2 with IC_{50} values in the range of 0.1–0.2 μM concentrations, while compounds showed weak inhibition of COX-1 as the IC_{50} values were 500-fold higher than that of COX-2 IC_{50} values. The most potent compound, 5-(4-chlorophenyl)-6-(4(methylsulfonyl)phenyl)-3-(methylthio)-1,2,4-triazine (**9c**) with the chloro atom at the *para* position of the phenyl ring, has a COX-1 IC_{50} value of 39.5 μM and COX-2 IC_{50} value of 0.10 μM with a selectivity index of 395 which is comparable to the selective COX-2 inhibitor celecoxib and its selectivity index of 405 (Table 1).

2.3. Docking simulation

In order to rationalize the observations of the biological activity of the synthesized compounds and provide more insights into the

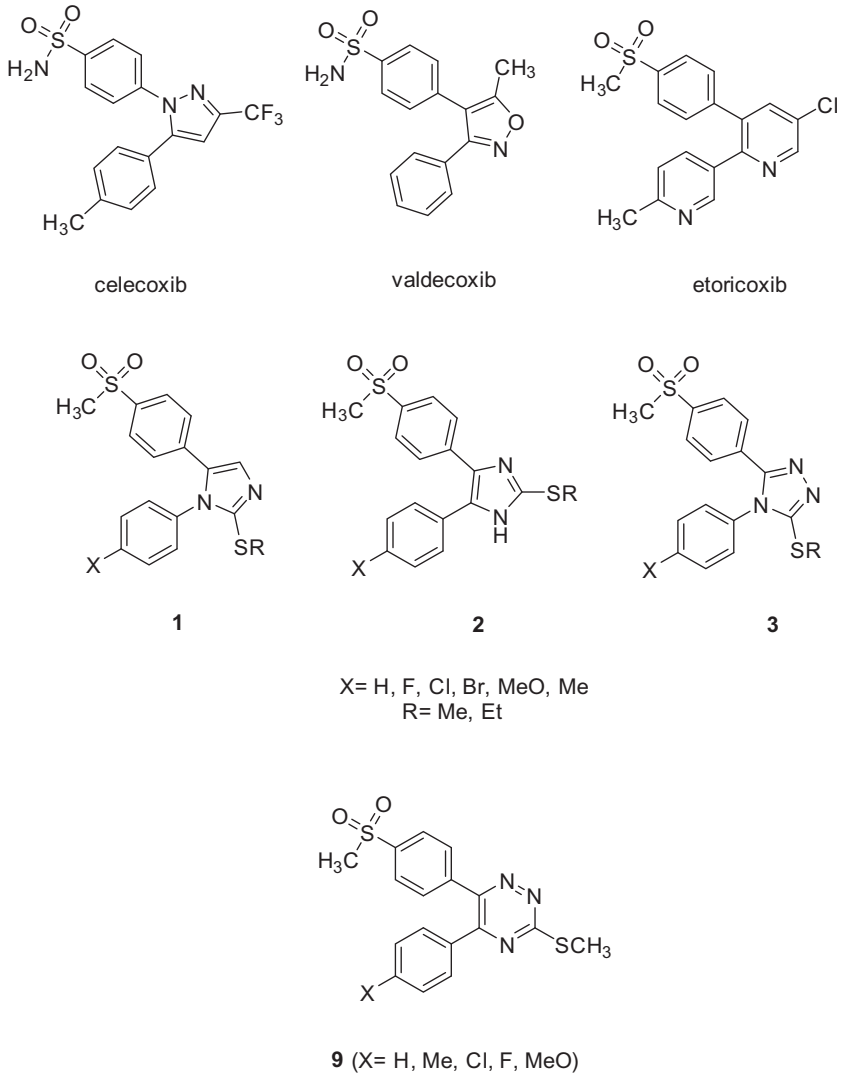

Figure 1. Representative of some marketed selective COX-2 inhibitors (celecoxib, valdecoxib and etoricoxib) and our previously reported ones (**1**–**3**). General structure of our newly synthesized compounds (**9**).

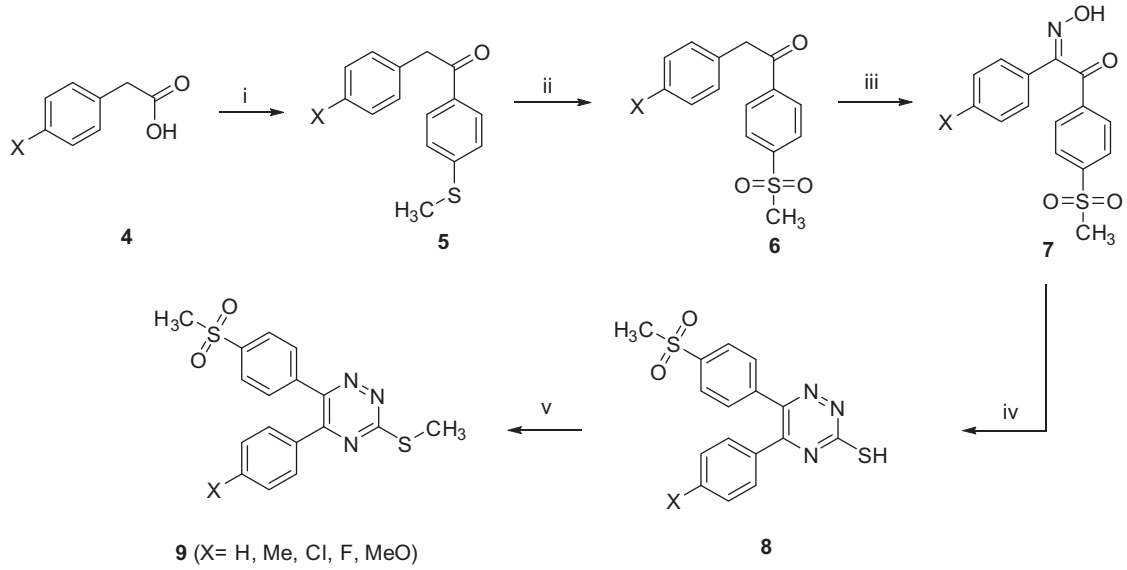

Scheme 1. Reagents and conditions: (i) Thioanisole, TFAA, H_3PO_4, rt, stir, 5 min; (ii) Oxone®, MeOH, THF, rt, stir, 4 h; (iii) (1) MeONa, MeOH, (2) BuONO, rt, stir; (iv) Thiosemicarbazide, H_2O, HCl, reflux; (v) CH_3I, Et_3N, CH_3OH, rt, stir.

Table 1
In vitro COX-1 and COX-2 enzyme inhibition data for the synthesized compounds

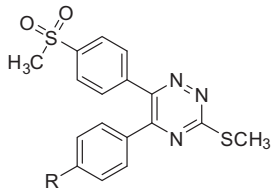

Compounds	R	IC_{50}[a] COX-1 (μM)	IC_{50}[a] COX-2 (μM)	Selectivity index[b]
9a	H	54.4	0.19	286.3
9b	CH_3	52.4	0.18	291.1
9c	Cl	39.5	0.10	395.0
9d	F	51.6	0.15	344.0
9e	CH_3O	50.1	0.17	294.7
Celecoxib		24.3	0.06	405.0

[a] The in vitro test compound concentration required to produce 50% inhibition of enzymatic activity.
[b] In vitro COX-2 selectivity index (COX-1 IC_{50}/COX-2 IC_{50}).

interactions, a molecular docking simulation of the representative compound **9c** was performed. Overall, the docking results were essentially in agreement with the biological data in terms of evaluation of interaction energy and binding mode. The protein-inhibitor complex obtained from docking simulation showed that the docked ligand was almost superimposed on the native co-crystallized one (SC-558) with RMSD being 0.136 and binding free energy of −10 kcal/mol. The hydrogen bonds and interactions between the docked ligand and the amino acids were the same as those between the native ligand SC-558 and the amino acids. In agreement with this statement, computational simulations revealed that the 4-chlorophenyl moiety of the ligand inhibitor (**9c**) was superimposed on the 4-bromophenyl group of the co-crystallized inhibitor SC-558, occupying the "hydrophobic pocket" constituted by the lipophilic and aromatic side chains of Phe381, Leu384, Tyr385, Trp387, Phe518 and Met522. Moreover, the 4-methylsulfonylphenyl moiety of compound (**9c**) similar to the 4-sulfonamidophenyl of SC-558 is located in a region of the active site called the 'selectivity site'. This site is surrounded by polar amino acid side chains of Arg518, Glu192, His90 and the backbone NH of Phe518. The oxygen atoms of the methylsulfonyl group of compound (**9c**) interacts through hydrogen bonds with the backbone NH group of Phe518 (2.9 Å) and with the guanidine group of Arg513 side chain (2.8 Å). Meanwhile, the N1 atom of triazine ring creates hydrogen bonding with the hydroxyl group of Tyr355 side chain (2.9 Å). Finally, the thiomethyl moiety of compound (**9c**) fills a space constituted by the aliphatic side chain of Leu359, Ile345, Leu531, V116, and interacts through van der Waals and hydrophobic contacts corresponding to the orientation of the trifluoromethyl group of the co-crystallized ligand SC-558. This space is oriented next to the 'classical NSAID's carboxylate bonding site' made mainly by Arg120 (Fig. 2).

As a consequence, the binding mode of compound **9c** is in high consistency with the results of the previously published

studies[15,16] and clearly explains and confirms the biologically obtained data tested on the COX-1/COX-2 enzymes.

2.4. 3D-QSAR study: k-Nearest Neighbour Molecular Field Analysis (kNN-MFA)

All the molecules were aligned based on the predefined substructure highlighted in Figure 3 comprising four atoms in the structure of SC-558. The aligned biologically active conformations of compounds were used for the calculation of molecular fields. Molecular fields are the steric, electrostatic and hydrophobic interaction energies which are used to develop a model for 3D-QSAR. Instead of calculating all three interaction fields together and making one model for all fields, one model was separately built for each field in order to investigate more precisely the lattice points around molecules.

Statistical parameters obtained for the three models are summarized in Table 2. The model selection criterion is the value of q^2 (cross validated r^2) and that of pred-r^2 (predictive r^2 for the test set).

Accordingly, a QSAR model is considered to be predictive if the following conditions are satisfied: $r^2 > 0.6$, $q^2 > 0.6$ and pred-$r^2 > 0.5$.[17,18] The q^2 and pred-r^2 values, which meet these conditions, for the three models based on the three different fields thus suggest that these models are useful tools for predicting COX-2 inhibitory activity.

Figures 4–6 show the contribution plot of the three models for the electrostatic, hydrophobic and steric fields respectively and indicate relative regions of the local fields around the aligned molecules leading to activity variation in the model. For electrostatic field, the lattice points generated in the model are E-985 (−10.0000, −10.0000), E-671 (2.8143, 3.1589), E-1138 (−0.9107, 0.0721) and E-453 (0.2156, 0.3351). These points suggested the significance of electrostatic properties as indicated in the ranges in parentheses for maximum COX-2 inhibitory activity. Similarly, the lattice points obtained for steric and hydrophobic fields are: S-951(−0.0111, −0.0105), S-388 (−0.0244, −0.0299) and S-4 (−0.0021, −0.0013) for steric, and H-644 (0.9968, 1.2361) and H-995 (0.2741, 0.4364) for hydrophobic. The high negative value for E-985 means that strong electron-withdrawing substituents in this region are favorable and would increase COX-2 inhibitory activity, as shown by the presence of sulfonamide and sulfonylmethyl groups in the most active compounds. Positive values for E-671 and E-453 show that electron-donating groups on the central ring B increase biological activity of compounds. There is

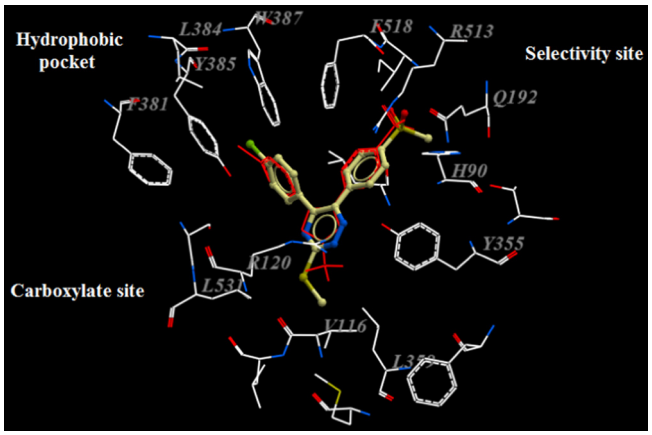

Figure 2. Docked conformation of (**9c**) (ball and stick) in the active site of COX-2. For clarity only amino acids within 7 Å distant from the docked ligand are shown. The co-crystallized ligand SC-558 (wire) in the active site is shown in red.

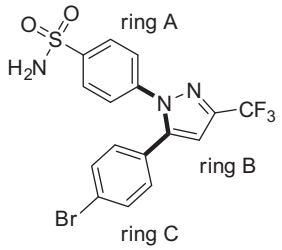

Figure 3. Scaffold used for alignment (SC-558). Bolded bonds represent the substructure used for alignment.

no electrostatic relationship between ring C and COX-2 inhibitory activity.

On the other hand, ring C might be substituted with either electron-withdrawing or electron-donating groups without loss of activity. Less bulky substituents are tolerated at rings A and C, meaning that increasing size of the groups substituted in these regions reduces COX-2 inhibitory activity, since S-388 and S-951 have negative values. The presence of bulky groups in the central ring B does not affect COX-2 inhibitory activity and there is no limitation regarding size of the group in this region. Positive values for the hydrophobic lattice points around ring A and ring C indicate that COX-2 inhibitory activity could be increased by substituting more hydrophobic groups in these two regions. However, there is no hydrophobicity relationship between ring B and biological activity. On the other hand, ring B may be substituted by hydrophilic groups without biological activity reduction; as in the classical NSAIDs, a hydrophilic carboxylate side chain exists.

Our synthesized compounds have similar potency (0.1–0.2 μM) due to little structural difference among them. The most active compound **9c** having a strong electron-withdrawing and hydrophobic group (methylsulfonyl) at ring A, an electron-donating group (methylthio) at ring B and a hydrophobic and less bulky group (chloro atom) at ring C strongly supports the above statements and results obtained by 3D-QSAR analysis.

Electron-withdrawing nature of the electronegative chloro atom does not contribute to the COX-2 inhibitory activity of the molecule. On the other hand, replacing chloro atom at ring C with electron-donating but still hydrophobic methyl and methoxy groups in compounds **9b** and **e** respectively, did not significantly reduce COX-2 inhibitory activity.

Regarding to structure–activity relationship (SAR) of our previous studies as well as resulted data in this research, different central heterocyclic rings such as imidazole, triazole, and triazine substituted with alkythio group, represented the promising potency and selectivity toward COX-2 enzyme. This research also indicated that expansion of central heterocyclic ring from azoles to triazine was tolerated by the target or even increased in selectivity and potency of some compounds like **9c**. In addition, in agreement of our studies, presence of more bulky and hydrophilic substituents like methoxy at ring C led to a decrease in COX-2 potency. On the other hand, more lipophilic halogens like chloro, and fluoro in this position retains the COX-2 inhibition activities.[10,11]

The 3D pharmacophore obtained by this docking simulation and 3D-QSAR study may be used for future drug developing projects for the design of selective COX-2 inhibitors (Fig. 7).

2.5. In vivo studies

Compounds (**9a**–**e**) were studied for determination of their potential AI in rat hind paw edema method; the results are presented in Table 3. The AI effects of the synthesized compounds were evaluated on the basis of the difference in hind paw thickness before

Table 2
Statistical results of 3D-QSAR study generated by forward–backward stepwise kNN-MFA method for selective COX-2 derivatives

Statistical parameters	Electrostatic field model	Steric field model	Hydrophobic field model
Training set size	66	68	69
Test set size	19	17	16
k nearest neighbour	6	3	9
q^2	0.8450	0.7144	0.6401
q^2-se	0.4615	0.6184	0.7373
Pred-r^2	0.6025	0.6947	0.6045
Pred-r^2se	0.7810	0.7184	0.6061
Degree of freedom	61	64	66
Selected descriptors	E_985	S_951	H_644
	E_671	S_388	H_995
	E_1138	S_4	
	E_453		

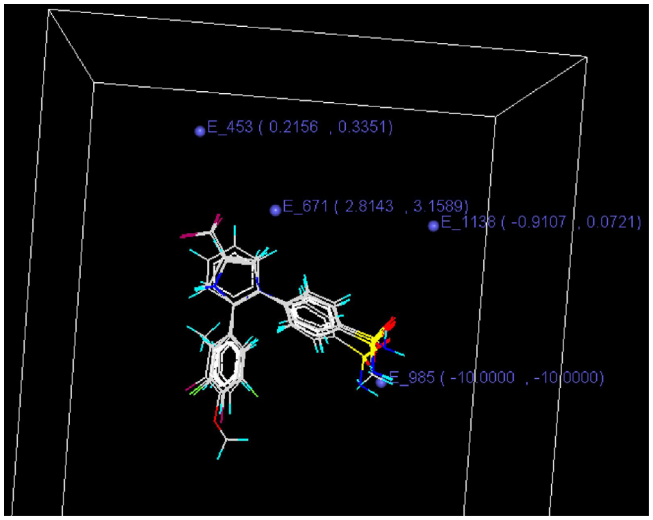

Figure 4. Contribution plot for electrostatic interactions around the superimposed molecular units of selective COX-2 inhibitors using SW kNN-MFA method.

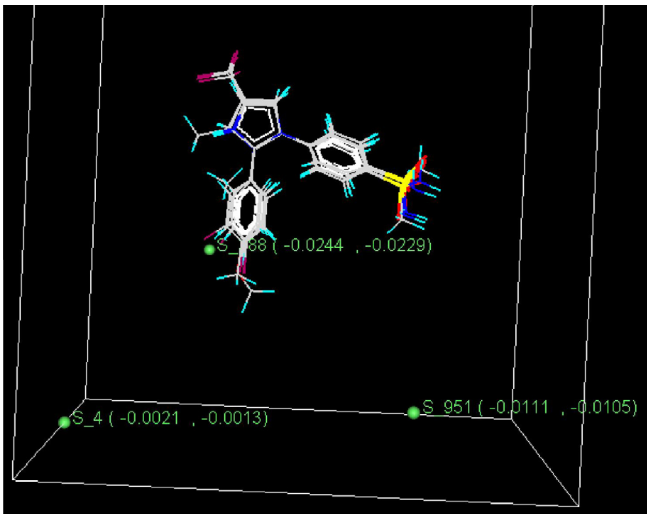

Figure 6. Contribution plot for steric interactions around the superimposed molecular units of selective COX-2 inhibitors using SW kNN-MFA method.

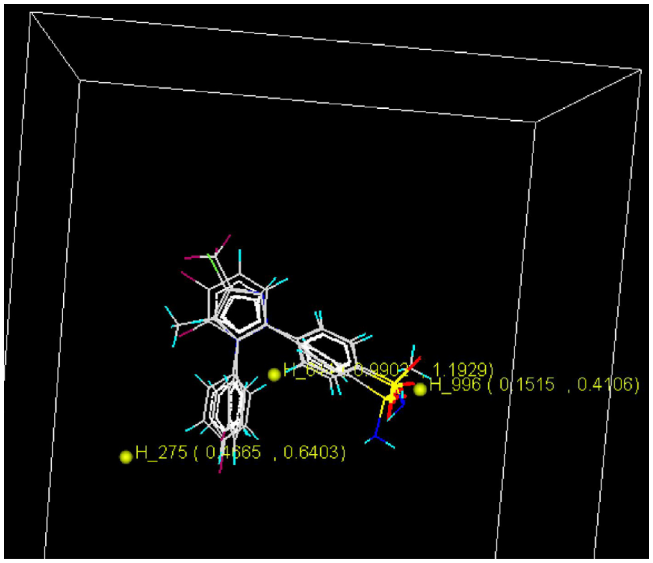

Figure 5. Contribution plot for hydrophobic interactions around the superimposed molecular units of selective COX-2 inhibitors using SW kNN-MFA method.

and after carrageenan injection as mm. As seen in Table 3, all compounds showed significant activity (p 0.01 or 0.05) compared to negative control at 1, 2 and 3 h after carrageenan injection in 3 and 6 mg/kg. Although, compound **9a** did not show any improvement in anti-inflammatory activity rather than indomethacin, other compounds revealed prominent anti-inflammatory activity in most cases at doses 3 and 6 mg/kg. Interestingly, compound **9c** not only was as strong as indomethacin (5 mg/kg) at dose of 3 mg/kg, but also showed more potency at dose of 6 mg/kg. Furthermore, compound **9e** at dose of 6 mg/kg was the most potent anti-inflammatory agent in this group and showed a significant difference with indomethacin (p 0.005) in 1 h after induction of edema. Almost all the AI properties of the all compounds are comparable to reference drug. AI activities of the tested compounds are in agreement with the observed data in the COX-2 inhibition assay.

Potential antinociceptive effects of the synthesized compounds were carried out using formalin-induced paw-licking test. Data is presented in Table 4 that shows mean licking time at two doses, 3 and 6 mg/kg for tested compounds and 5 mg/kg for indomethacin. In both early and late phases of pain response, most of the compounds showed significant antinociceptive activity compared to negative control. The analgesic activity of synthesized compound was considerable in the first or second phase of nociception in comparison of reference molecule indomethacin.

3. Conclusion

In the present study, novel 5-Aryl-6-(4-methylsulfonyl)-3-(metylthio)-1,2,4-triazine compounds were synthesized and biologically evaluated against COX-1/COX-2 inhibitory activity

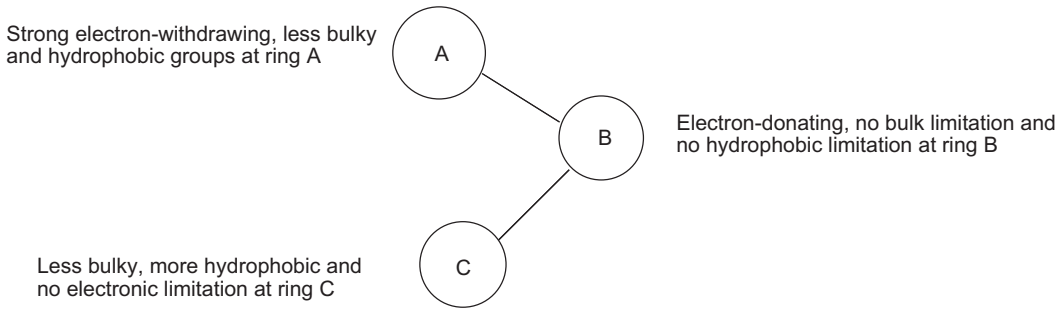

Figure 7. 3D-pharmacophore obtained by k-Nearest Neighbour Molecular Field Analysis.

Table 3
Anti-inflammatory effects of the test compound on carrageenan-induced hind paw edema

Compounds	Dose (mg/kg)	Difference in hind paw thickness before and after carrageenan injection (mm)		
		1 h After inj.	2 h After inj.	3 h After inj.
9a	3	1.45 ± 0.08[N]	1.77 ± 0.31	1.19 ± 0.12[N,M]
	6	1.09 ± 0.14[N,M]	0.94 ± 0.13[N,M]	0.83 ± 0.18[N,M]
9b	3	0.87 ± 0.39[N,M]	0.68 ± 0.31[N,M]	0.55 ± 0.3[N,M]
	6	0.98 ± 0.16[N,M]	0.8 ± 0.16[N,M]	0.67 ± 0.2[N,M]
9c	3	1 ± 0.31[N,M]	0.71 ± 0.41[N,M]	0.54 ± 0.35[N,M]
	6	0.89 ± 0.3[N,M]	0.58 ± 0.31[N,M]	0.41 ± 0.26[N,M]
9d	3	1.24 ± 0.18[N,M]	1.16 ± 0.22[N,M]	0.97 ± 0.29[N,M]
	6	0.75 ± 0.26[N,M]	0.56 ± 0.19[N,M]	0.34 ± 0.12[N,M]
9e	3	0.96 ± 0.35[N,M]	0.72 ± 0.4[N,M]	0.64 ± 0.36[N,M]
	6	0.58 ± 0.15[N,M,P]	0.43 ± 0.13[N,M]	0.3 ± 0.1[N,M]
Neg. Cont.		1.84 ± 0.41	1.86 ± 0.38	1.78 ± 0.39
Indomethacin	5	1.05 ± 0.14[N,M]	0.81 ± 0.22[N,M]	0.57 ± 0.25[N,M]

Data obtained from experiments were expressed as mean ± sd, $n = 6$.
[N] Significant difference with negative control (p value 0.05).
[M] Significant difference with negative control (p value 0.01).
[P] Significant difference with negative control (p value 0.005).

Table 4
Effects of the test compounds on nociceptive response formalin test

Compounds	Dose (mg/kg)	Licking time after formalin injection in early and late phases (second)	
		1st phase	2nd phase
9a	3	57 ± 11[N]	133 ± 61.5[N]
	6	58 ± 10[N]	155 ± 38
9b	3	49 ± 14.5[N,M]	175 ± 36.5
	6	61 ± 17	139 ± 42[N]
9c	3	30 ± 6.6[N,M]	85 ± 26.6[N,M]
	6	37 ± 6[N,M]	140 ± 36.5[N]
9d	3	52 ± 11[N,M]	127 ± 49.5[N]
	6	34 ± 11.5[N,M]	152 ± 32.5
9e	3	46 ± 5.5[N,M]	227 ± 84
	6	49 ± 10[N,M]	118 ± 34[N,M]
Neg. Cont.		80 ± 19	217 ± 68.5
Indomethacin	5	45 ± 10[N,M]	127 ± 21[N,M]

Data obtained from experiments were expressed as mean ± sd, $n = 6$.
[N] Significant difference with negative control (p value 0.05).
[M] Significant difference with negative control (p value 0.01).

which led to the finding of a potent and selective COX-2 inhibitor, 5-(4-Chlorophenyl)-6-(4-(methylsulfonyl)phenyl)-3-(methylthio)-1,2,4-triazine (**9c**) with IC_{50} = 0.10 μM and selectivity index of 395 almost comparable to celecoxib (SI = 405), which could be considered as a new lead for further drug development. Furthermore, docking simulation performance on our lead compound (**9c**) gave satisfactory results and could prove its potential capability to inhibit COX-2. As well, the chemical structure of our new compound (**9c**) was in high consistency with the 3D-pharmacophore model obtained from 3D-QSAR study on a set of selective COX-2 inhibitors.

Our results demonstrated that diaryl-triazine scaffolds act as in vitro COX-2 inhibitors as well as in vivo analgesic and AI agents. This study shows that new analogous of diaryltriazine present a promising lead for generation of new AI and analgesic agents.

4. Experimental

4.1. Chemistry

All commercially available reagents were purchased from Merck AG, Aldrich or Acros Organics and used without further

purification. Column chromatography was carried out on silica gel (230–400 mesh). TLC was conducted on silica gel F254 plates. Melting points were measured on a Kofler hot stage apparatus and are uncorrected. The IR spectra were taken using Nicolet FT-IR Magna 550 spectrographs (KBr disks). Mass spectra of the products were obtained with an HP (Agilent technologies) 5937 Mass Selective Detector. ^{1}H NMR spectra were recorded on a Bruker 500 MHz and ^{13}C NMR spectra on a Bruker 100 MHz NMR instruments. The chemical shifts (δ) and coupling constants (J) are expressed in parts per million and hertz, respectively. Elemental analyses were carried out by a CHN-Rapid Heraeus elemental analyzer. The results of elemental analyses (C, H, N) were within ±0.4% of the calculated values.

4.1.1. General procedure for the preparation of compounds 9

1 equiv of 5-Aryl-6-(4-(methylsulfonyl) phenyl)-1,2,4-triazine-3-thiol (**8**), 1.2 equiv of methyl iodide and 1.5 equiv of triethylamine were added to dry methanol and the mixture was stirred for 30 min. It was concentrated under reduced pressure, diluted with dichloromethane and washed with ammonium chloride solution and decanted from aqueous layer. Organic phase was dried over sodium sulfate, filtered and concentrated under vacuum. It was chromatographed on silica gel (230–400 mesh) using dichloromethane/methanol (5%) as eluent.

4.1.1.1. 6-(4-(Methylsulfonyl)phenyl)-3-(methylthio)-5-phenyl-1,2,4-triazine (9a). Yield = 85%; mp = 218–220 °C; ^{1}H NMR (500 MHz, $CDCl_3$) δ: 2.79 (s, 3H. SCH_3), 3.10 (s, 3H, SO_2CH_3), 7.39 (t, J = 7.5 Hz, 2H, $H_{3,5}$-Ar_5), 7.51 (dd, J = 7.5 Hz, 3H, $H_{2,4,6}$-Ar_5), 7.75 (d, J = 8.0 Hz, 2H, $H_{2,6}$-Ar_6), 7.95 (d, J = 8.0 Hz, 2H, $H_{3,5}$-Ar_6); ^{13}C NMR (100 MHz, $CDCl_3$) δ: 13.96, 44.44, 127.67, 128.89, 129.77, 130.27, 131.40, 134.45, 140.98, 141.07, 151.95, 155.60, 172.29; IR (KBr) ν cm^1: 1153, 1301 (SO_2CH_3), 1487(C=N, triazine); MS, m/z (%) 357 (M^+, 10), 256 (100), 193 (36), 176 (43), 151 (17), 88 (7). Anal. Calcd for $C_{17}H_{15}N_3O_2S_2$: C, 57.12; H 4.23; N, 11.76, Found: C, 57.07; H, 4.19; N, 11.94.

4.1.1.2. 6-(4-(Methylsulfonyl)phenyl)-3-(methylthio)-5-(p-tolyl)-1,2,4-triazine (9b). Yield: 80%; mp = 223–225 °C; ^{1}H NMR (500 MHz, $CDCl_3$) δ: 2.41 (s, 3H, Ar-CH_3), 2.77 (s, 3H, SCH_3), 3.11 (s, 3H, SO_2CH_3), 7.17 (d, J = 7.5 Hz, 2H, $H_{3,5}$-Ar_5), 7.42 (d, J = 7.5 Hz, 2H, $H_{2,6}$-Ar_5), 7.76 (d, J = 7.85 Hz, 2H, $H_{2,6}$-Ar_6), 7.95 (d, J = 7.85 Hz, 2H, $H_{3,5}$-Ar_6); ^{13}C NMR (100 MHz, $CDCl_3$) δ: 13.93, 21.52, 44.45, 127.66, 129.63, 129.80, 130.23, 131.48, 140.97, 141.26, 142.17, 151.87, 155.57, 172.13; IR (KBr) ν cm^1: 1157, 1316 (SO_2CH_3), 1495 (C=N, triazine); MS, m/z (%) 371 (M^+, 10), 270 (100), 207 (30), 189 (30), 165 (6), 73 (5). Anal. Calcd for $C_{18}H_{17}N_3O_2S_2$: C, 58.20; H 4.61; N, 11.36, Found: C, 58.09; H, 4.39; N, 11.44.

4.1.1.3. 5-(4-Chlorophenyl)-6-(4-(methylsulfonyl)phenyl)-3-(methylthio)-1,2,4-triazine (9c). Yield: 80%; mp = 148–150 °C; ^{1}H NMR (500 MHz, $CDCl_3$) δ: 2.78 (s, 3H, SCH_3), 3.11 (s, 3H, SO_2CH_3), 7.37 (d, J = 8.1 Hz, 2H, $H_{3,5}$-Ar_5), 7.48 (d, J = 8.1 Hz, 2H, $H_{2,6}$-Ar_5), 7.75 (d, J = 7.95 Hz, 2H, $H_{2,6}$-Ar_6), 7.98 (d, J = 7.95 Hz, 2H, $H_{3,5}$-Ar_6); ^{13}C NMR (100 MHz, $CDCl_3$) δ: 13.96, 44.42, 127.84, 129.27, 130.23, 131.13, 132.82, 137.99, 140.67, 141.31, 151.71, 154.36, 172.36; IR (KBr) ν cm^1: 1149, 1304 (SO_2CH_3), 1479 (C=N, triazine); MS, m/z (%) 393 (M^++2, 3), 391 (M^+, 10), 290 (100), 227 (34), 211 (28), 176 (57), 150 (10), 75 (9). Anal. Calcd for $C_{17}H_{14}ClN_3O_2S_2$: C, 52.10; H 3.60; N, 10.72, Found: C, 52.35; H, 3.47; N, 10.59.

4.1.1.4. 5-(4-Fluorophenyl)-6-(4-(methylsulfonyl)phenyl)-3-(methylthio)-1,2,4-triazine (9d). Yield: 90%; mp = 168–170 °C; ^{1}H NMR (500 MHz, $CDCl_3$) δ: 2.78 (s, 3H, SCH_3), 3.12 (s, 3H, SO_2CH_3), 7.08 (t, J = 8.2 Hz, 2H, $H_{3,5}$-Ar_5), 7.55 (m, 2H, $H_{2,6}$-Ar_5), 7.75 (d, J = 7.9 Hz, 2H, $H_{2,6}$-Ar_6), 7.97 (d, J = 7.9 Hz, 2H, $H_{3,5}$-Ar_6); ^{13}C NMR (100 MHz, $CDCl_3$) δ: 13.96, 44.42, 116.25 (d, J = 21.9 Hz), 127.81, 130.21, 130.48, 132.12 (d, J = 8.79 Hz), 141.06 (d, J = 39.97 Hz), 151.74, 154.38, 164.60 (d, J = 252.45), 172.26; IR (KBr) ν cm^1: 1149, 1301 (SO_2CH_3), 1487 (C=N, triazine); MS, m/z (%) 375 (M^+, 12), 274 (100), 211 (36), 195 (35), 175 (12). Anal. Calcd for $C_{17}H_{14}FN_3O_2S_2$: C, 54.38; H 3.76; N, 11.23, Found: C, 54.53; H, 3.42; N, 11.44.

4.1.1.5. 5-(4-Methoxyphenyl)-6-(4-(methylsulfonyl)phenyl)-3-(methylthio)-1,2,4-triazine (9e). Yield: 90%; mp = 173–175 °C; ^{1}H NMR (500 MHz, $CDCl_3$) δ: 2.77 (s, 3H, SCH_3), 3.12 (s, 3H, SO_2CH_3), 3.85 (s, 3H, OCH3), 6.87 (d, J = 8.45 Hz, 2H, $H_{3,5}$-Ar_5), 7.51 (d, J = 8.45, 2H, $H_{2,6}$-Ar_5), 7.78 (d, J = 8.0 Hz, 2H, $H_{2,6}$-Ar_6), 7.97 (d, J = 8.0 Hz, 2H, $H_{3,5}$-Ar_6); ^{13}C NMR (100 MHz, $CDCl_3$) δ: 13.93, 44.46, 55.48, 114.36, 126.27, 127.75, 130.15, 131.76, 140.95, 141.58, 151.63, 154.92, 162.39, 171.93; IR (KBr) ν cm^1 1155, 1313 (SO_2CH_3), 1485 (C=N, triazine); MS, m/z (%) 387 (M^+, 20), 286 (100), 223 (11), 207 (40), 163 (15), 73 (10). Anal. Calcd for $C_{18}H_{17}N_3O_3S_2$: C, 55.80; H 4.42; N, 10.84 Found: C, 55.64; H, 4.48; N, 10.68.

4.2. Docking simulation method

COX-2 atomic coordinates in complex with the selective COX-2 inhibitor SC-558 with ID number: 1CX2 was retrieved from Brookhaven Protein Data Bank. To set the initial coordinates for the docking simulation, all water molecules, *N*-acetyl-D-glucosamine residues and chains B, C and D were removed and excluded from all calculations. The remaining chain A was considered for the following calculations. Ligand structure was sketched using MarvinSketch and geometry optimized using semiempirical AM1 method in Gaussian98. The resulting minimized conformation was then submitted to molecular docking simulation. Docking calculations were performed with the program AutoDock Vina. AutoDockTools 1.5.4 was used to visualize, add polar hydrogens and Kollman partial charges to the protein and to define rotatable bonds for the inhibitor ligand. Active site was defined by a grid point spacing of 1 A and 20 × 20 × 20 points were used. The grid was centered on the mass center of the crystallographic inhibitor SC-558 (X = 24.26, Y = 21.53, Z = 16.5).

A molecular mechanical/energy minimization approach was performed to refine the AutoDock output. Such a structural optimization of the complex obtained was necessary because the docking software AutoDock does not perform any structural optimization of the complexes found. The computational protocol applied consisted in the application of Amber force field in Gaussian 98. Moreover, due to the large number of atoms in the COX-2/inhibitor complex obtained by docking, a subset comprising only the inhibitor and a shell of residues 6 A distant from the inhibitor was created and submitted to energy minimization.[19] After docking calculation and energy minimization, the best pose with the lowest free energy of binding (ΔG) was used for investigating the binding mode and possible interactions between ligand and amino acids in the COX-2 active site.

4.3. k-Nearest neighbour molecular field analysis

A data set comprising 88 selective COX-2 inhibitors belonging to three chemical classes (triaryl rings, 1,3-diarylcycloalkanopyrazoles and diphenylhydrazids) with reported COX-2 enzymatic activity (IC_{50}) were taken from literature.[20] The 3D-QSAR study was performed using QSARPro software. 2D and 3D structure of compounds were sketched and geometrically optimized with the Merck Molecular Force Field (MMFF) method taking the root mean

square gradient (RMS) of 0.01 kcal/mol and iteration limit to 10,000. Steric, electrostatic and hydrophobic fields were computed at each grid point considering Gasteiger-Marsili charges. Methyl probe of charge +1 with 10.0 kcal/mol electrostatic and 30.0 kcal/mol steric cut-off were used for field's generation. A value of 1.0 is assigned to the distance-dependent dielectric constant. After calculating the descriptors, constant and near constant descriptors were removed and excluded from calculations. Training and test sets were generated using sphere exclusion method. Among the various methods in variable selection and model development, stepwise forward–backward variable selection method was used for data reduction and k-Nearest neighbor (kNN) method was chosen for model development.[21]

4.4. In vitro cyclooxygenase (COX) inhibition assays

The assay was performed using an enzyme chemiluminescent kit (Cayman chemical, MI, USA) according to our previously reported method.[22] The Cayman chemical chemiluminescent COX (ovine) inhibitor screening assay utilizes the heme-catalyzed hydroperoxidase activity of ovine cyclooxygenases to generate luminescence in the presence of a cyclic naphthalene hydrazide and the substrate arachidonic acid. Arachidonate-induced luminescence was shown to be an index of real-time catalytic activity and demonstrated the turnover inactivation of the enzyme. Inhibition of COX activity, as measured by luminescence, by a variety of selective and nonselective inhibitors showed potencies similar to those observed with other in vitro and whole cell methods.

4.5. In vivo anti-inflammatory and analgesic evaluation

4.5.1. Materials and methods

4.5.1.1. Animals. Adult male, Swiss albino mice (25–30 g) were used for antinociceptive activities of the compounds. For AI study, adult male Wistar rats (120–160 g) were used. All animals were housed at room temperature and 50–55% relative humidity, with 12 h light/dark cycle. Standard rodent diet and water were used for animal feeding. Animals were acclimatized to the laboratory environment for at least 12 h before the experiment. The protocols adopted for the animal experiment were approved by the institutional animal ethics committee, part of the research ethics authorities at Tehran University of Medical Sciences.

4.5.1.2. Chemical and drug administration. Indomethacin was used in AI and antinociceptice study as positive control. Animals were divided into 7 groups as control group, reference group and test groups (1–5). The control group received solvent (DMSO + tween 20) since test compounds and indomethacin were dissolved in DMSO + tween 20. Each group included 6 animals for evaluation. Test groups received the synthesized compounds (**9a**–**e**) in concentration of 3 and 6 mg/kg both for AI and antinociceptive activity investigation.

4.5.2. Rat hind paw edema method

The anti-inflammatory activity of the test compound was evaluated by the carrageenan paw edema method in rat.[23] The test compounds at concentrations of 3 and 6 mg/kg and indomethacin at 5 mg/kg were administration as intraperitoneal injection (IP). Thirty minutes after the IP injection of samples, reference drug and dosing vehicle (50 μL/100 g), each rat was injected with freshly prepared solution of carrageenan (50 μL, 2.5% w/v), into sub-plantar tissue of the right hind paw. Paw edema was measured at 0, 60, 120 and 180 min. after carrageenan injections. The difference in hind paw thickness was measured by a Vernier caliper. Mean values of each treated group were compared with control group and analyzed by statistical methods.

4.5.3. Analgesic activity

The analgesic activities of the test compounds were evaluated by formalin test. The animals were fixed in a partial restraint 30 min after IP injection of test compound at concentrations of 3 and 6 mg/kg. For positive control, indomethacin at concentration of 5 mg/kg was used. The experimental animals were assigned to seven groups, with 6 mice in each group. The formalin test was conducted based on the reported procedures.[24] For the formalin test, groups of animals received the solvent (DMSO + tween 20) as control, reference drug (indomethacin) and test groups at two doses, 3 and 6 mg/kg. After 30 min, 50 μL of 2.5% formalin in normal saline was injected into the sub-plantar right hind paw to each animal. The duration of paw licking was used as an index to determine painful response. Neurogenic period (initial phase) and inflammatory period (secondary phase) were described at 0–5 min and 15–60 min after formalin injection respectively.

4.6. Statistical analysis

Statistical evaluations of the data obtained from 6 animals for each group were performed using Graph Pad Prism 5. One-way analysis of variance (ANOVA) was used for evaluation of statistical differences between groups. For comparison of data with others, Newman–Keuls multiple comparison tests was used and statistical significance at a level of $p < 0.05$, < 0.01, and < 0.005 was considered.

Acknowledgment

This research has been supported by Tehran University of Medical Sciences Health Services Grant No. 7950.

Supplementary data

Supplementary data associated with this article can be found, in the online version, at http://dx.doi.org/10.1016/j.bmc.2013.12.002.

References and notes

1. Warner, T. D.; Giuliano, F.; Vojnovic, I.; Bukasa, A.; Mitchell, J. A.; Vane, J. R. *Natl. Acad. Sci. U.S.A.* **1999**, *96*, 7563.
2. Simmons, D. L.; Botting, R. M.; Hla, T. *Pharmacol. Rev.* **2004**, *56*, 387.
3. Vane, J. R.; Botting, R. M. *Inflamm. Res.* **1998**, *S78*, 47.
4. Khan, A. A.; Iadarola, M.; Yang, H. Y.; Dionne, R. A. J. *Pain* **2007**, *8*, 349.
5. Kojima, F.; Kapoor, M.; Kawai, S.; Crofford, L. J. *Expert Rev. Clin. Immunol.* **2006**, *2*, 277.
6. Sarkar, F. H.; Adsule, S.; Li, Y.; Padhye, S. *Mini Rev. Med. Chem.* **2007**, *7*, 599.
7. Nivsarkar, M.; Banerjee, A.; Padh, H. *Pharmacol. Rep.* **2008**, *60*, 692.
8. White, W. B.; Faich, G.; Borer, J. S.; Makuch, R. W. *Am. J. Cardiol.* **2003**, *92*, 411.
9. Grosser, T.; Fries, S.; FitzGerald, G. A. *J. Clin. Invest.* **2006**, *116*, 4.
10. a) Navidpour, L.; Shadnia, H.; Shafaroodi, H.; Amini, M.; Dehpour, A. R.; Shafiee, A. *Bioorg. Med. Chem.* **1976**, *2007*, 15; b) Assadieskandar, A.; Amirhamzeh, A.; Salehi, M.; Ozadali, K.; Ostad, S. N.; Shafiee, A.; Amini, M. *Bioorg. Med. Chem.* **2013**, *21*, 2355.
11. Navidpour, L.; Shafaroodi, H.; Abdi, K.; Amini, M.; Ghahremani, M. H.; Dehpour, A. R.; Shafiee, A. *Bioorg. Med. Chem.* **2006**, *14*, 2507.
12. Veeramaneni, V. R.; Pal, M.; Yeleswarapu, K. R. *Tetrahedron* **2003**, *59*, 3283.
13. Irannejad, H.; Amini, M.; Khodagholi, F.; Ansari, A.; Khoramian Tusi, S.; Sharifzadeh, M.; Shafiee, A. *Bioorg. Med. Chem.* **2010**, *18*, 4224.
14. Ansari, N.; Khodagholi, F.; Ramin, M. R.; Amini, M.; Irannejad, H.; Dargahi, L.; Dehghani Amirabad, A. *Neurochem. Inter.* **2010**, *57*, 958.
15. Biava, M.; Porretta, G. C.; Poce, G.; Supino, S.; Cappelli, A.; Vomero, S.; Manetti, F.; Botta, M.; Sautebin, L.; Rossi, A.; Ghelardini, C.; Vivoli, E.; Makovec, F.; Anzellotti, P.; Patrignani, P.; Anzini, M. *J. Med. Chem.* **2007**, *50*, 5403.
16. Unsal-Tan, O.; Ozadali, K.; Piskin, K.; Balkan, A. *Eur. J. Med. Chem.* **2012**, *57*, 59.
17. Golbraikh, A.; Tropsha, A. *J. Mol. Graph. Model.* **2002**, *20*, 269.

18. Afantitis, A.; Melagraki, G.; Sarimveis, H.; Igglessi-Markopoulou, O.; Kolliasnovel, G. A *Eur. J. Med. Chem.* **2009**, *44*, 877.
19. Anzini, M.; Rovini, M.; Cappelli, A.; Vomero, S.; Manetti, F.; Botta, M.; Sautebin, L.; Rossi, A.; Ghelardini, C.; Norcini, M.; Giordani, A.; Makovec, F.; Anzellotti, P.; Patrignani, P.; Biava, M. *J. Med. Chem.* **2008**, *51*, 4476.
20. Kim, H. J.; Chae, C. H.; Yi, K. Y.; Park, K. L.; Yoo, S. E. *Bioorg. Med. Chem.* **2004**, *12*, 1629.
21. Sharma, M. C.; Kohli, D. V. *Med. Chem. Res.* **2012**, *21*, 2837.
22. Zarghi, A.; Najafnia, L.; Daraie, B.; Dadrass, O.; Hedayati, M. *Bioorg. Med. Chem. Lett.* **2007**, *17*, 5634.
23. Kupeli, E.; Tatli, I. I.; Akdemir, Z. S.; Yesilada, E. *J. Ethnopharmcol.* **2007**, *114*, 234.
24. Meunier, C. J.; Burton, J.; Cumps, J.; Verbeeck, R. K. E. *J. Pharm. Sci.* **1998**, *6*, 307.